Technical Notes

TECHNICAL NOTES are short manuscripts describing new developments or important results of a preliminary nature. These Notes cannot exceed 6 manuscript pages and 3 figures; a page of text may be substituted for a figure and vice versa. After informal review by the editors, they may be published within a few months of the date of receipt. Style requirements are the same as for regular contributions (see inside back cover).

Computation of Unsteady Laminar Boundary Layers Subject to Traveling-Wave Freestream Fluctuations

R. L. Evans*
University of British Columbia, Vancouver, British Columbia, Canada

Nomenclature

B = freestream velocity amplitude factor
P = pressure
Q = traveling-wave convection velocity
t = time
u = velocity in the boundary layer
Δu = amplitude of boundary-layer velocity
Ue = velocity at outer edge of the boundary layer
ΔUe = amplitude of velocity at the bounary-layer edge
U_0 = mean freestream velocity
x = distance from leading edge
y = coordinate normal to surface
η = similarity parameter, $(U_0/\nu x)^{1/2}y$
ν = kinematic viscosity
ρ = fluid density
ϕ = phase shift relative to freestream velocity
ϕ_τ = wall-shear-stress phase shift
ω = radian frequency
$\bar{\omega}$ = reduced frequency, $\omega x/U_0$

Introduction

An unsteady boundary layer may develop because of either standing-wave or traveling-wave fluctuations in the freestream. A standing-wave type of freestream fluctuation occurs when the perturbations in the freestream are everywhere in phase, as might happen when an aircraft wing experiences a sudden change in angle of attack. The traveling-wave type of fluctuation occurs when a disturbance is convected in the freestream, as in turbomachinery when the wakes of upstream blades are convected over a downstream blade row, as shown by Evans.[1] In this Note, simple modifications to the boundary conditions for a well-known unsteady boundary-layer calculation method are developed to accomodate both standing-wave and traveling-wave freestream fluctuations. Calculations using the modified procedure are presented for both types of fluctuation, and comparison is made with available experimental and analytical results.

Calculation Method

The calculation method used is a modified version of that developed by Cebeci and Carr.[2] In its original form, however, the calculation procedure was only suitable for standing-wave freestream fluctuations, with the freestream velocity given by

$$Ue(t) = U_0(1 + B\cos\omega t) \tag{1}$$

To accommodate traveling-wave freestream conditions, the program was modified to allow the freestream velocity to be of the form

$$Ue(x,t) = U_0[1 + B\cos\omega(t - x/Q)] \tag{2}$$

where Q is the traveling wave convection velocity. Equation (2) was used to provide the freestream velocity distribution and was differentiated in order to formulate the freestream pressure variation.

The freestream pressure gradient may be found from the unsteady Bernoulli equation

$$-\frac{1}{\rho}\frac{\partial P}{\partial x} = \frac{\partial Ue}{\partial t} + Ue\frac{\partial Ue}{\partial x} \tag{3}$$

If the freestream velocity given by Eq. (2) is used in Eq. (3), then the external pressure gradient, which is felt across the complete boundary layer, is given by

$$-\frac{1}{\rho}\frac{\partial P}{\partial x} = \left(1 - \frac{U_0}{Q}\right)\omega B U_0 \cos\omega\left(t - \frac{x}{Q}\right) \tag{4}$$

and the behavior of the boundary layer can be seen to be critically dependent on the traveling-wave convection velocity ratio Q/U_0.

For large values of traveling-wave convection velocity Q, the right-hand side of Eq. (4) reverts to the situation where the pressure gradient is everywhere in phase in the freestream, and the boundary layer behavior is the same as with a standing-wave freestream perturbation. With $Q/U_0 = 1.0$, the right-hand side of Eq. (4) disappears altogether, and there is no freestream pressure gradient. Very little phase shift is expected in this case, although the freestream boundary conditions must still be met. Finally, for $Q/U_0 < 1.0$, the right-hand side of Eq. (4) is negative, resulting in a freestream pressure gradient that lags in phase behind the freestream velocity. This, in turn, results in a phase lag in the boundary-layer velocity, and this phase lag can be expected to increase with decreasing values of Q/U_0.

The program output procedure also was changed to provide the amplitude fluctuation ratio $\Delta u/\Delta Ue$ and the phase shift through the boundary layer at each x station rather than the in-phase and out-of-phase components of velocity. It was felt that this provided better physical insight into unsteady boundary-layer behavior. With these modifications, the program was found to converge and to provide solutions over a wide range of reduced frequency $\bar{\omega}$ and convection velocity Q. The program provided identical results to the original Cebeci and Carr version when a value of Q/U_0 greater than about 100 was used.

Results

Initial calculations were conducted for a laminar boundary layer developing on a flat plate in air with standing-wave freestream conditions. The freestream velocity was 157 ft/s, the fluctuation amplitude 10%, and the frequency 0.25 Hz. Figure 1 shows the results of calculations for a reduced frequency of 0.2 and 0.4 compared to the analytical solution of Lighthill.[3] The amplitude fluctuation ratio $\Delta u/\Delta Ue$ and the phase shift ϕ through the boundary layer are shown as a function of the boundary-layer similarity parameter η. The

Received March 3, 1988; revision received Nov. 17, 1988. Copyright © 1989 American Institute of Aeronautics and Astronautics, Inc. All rights reserved.

*Associate Professor, Department of Mechanical Engineering.

phase lead results from the velocity in the inner part of the layer responding more readily to the changing pressure level in the boundary layer because of the lower velocity there.

Caculations for a traveling-wave type of freestream fluctuation are shown in Fig. 2, in comparison with the experimental data of Patel.[4] The calculations compare quite favorably with the experimental data, with the phase shift throughout the boundary layer now a phase lag, rather than a phase lead as for standing-wave freestream fluctuations. Figure 3 shows the results of calculations for a reduced frequency of 0.5 and four values of Q/U_0. For $Q/U_0<1.0$, the amplitude ratio is less then 1.0 in the outer portion of the layer, and the peak moves toward the wall. The phase shift turns from negative to positive as the convection velocity ratio is increased and eventually reaches the standing-wave freestream value as $Q/U_0\to\infty$. This behavior is entirely consistent with the change in sign of the freestream pressure gradient, as predicted by Eq. (4). A summary of the wall-shear phase shift as a function of the reduced frequency is shown in Fig. 4. For $Q/U_0>1.0$, the inertia term in the equations of motion dominates, and there is a phase lead that increases with increasing reduced frequency. For $Q/U_0<1.0$, the convection term dominates, and a phase lag that increases with increasing reduced frequency results. Further details of the calculation method and more extensive results are given in the report by Evans.[5]

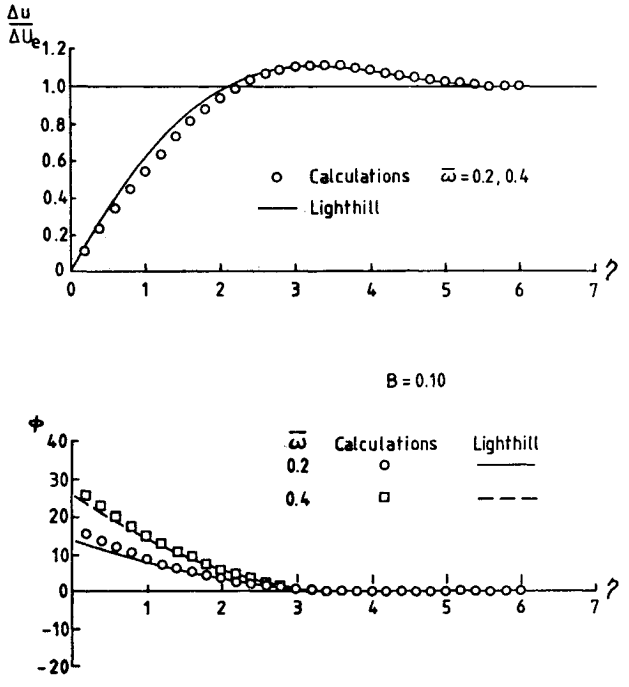

Fig. 1 Standing-wave freestream calculations compared to theory of Lighthill.

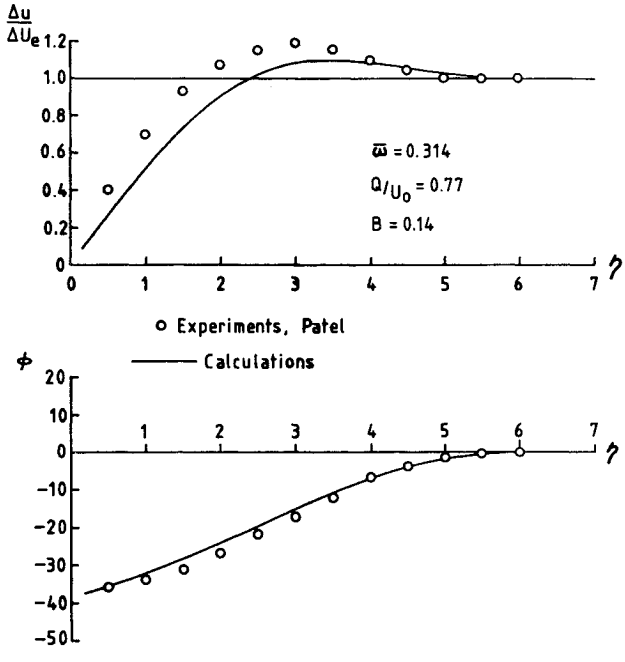

Fig. 2 Traveling-wave freestream calculations compared to experiments of Patel.

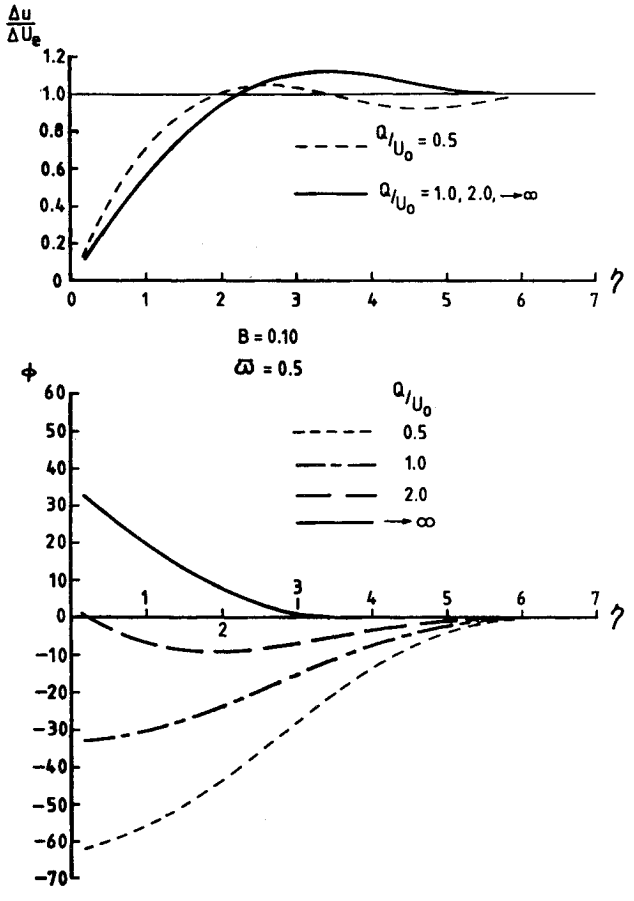

Fig. 3 Traveling-wave freestream calculations for a range of the convection velocity ratio.

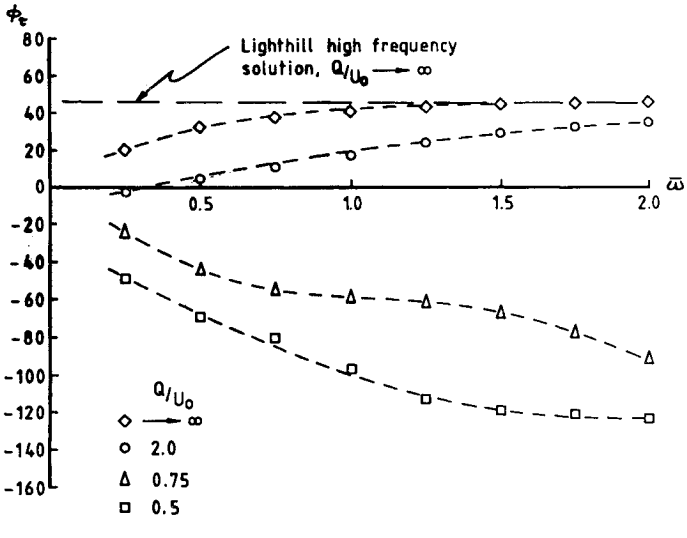

Fig. 4 Wall-shear phase shift as a function of reduced frequency.

Conclusions

Unsteady laminar boundary layers exhibit quite different behavior, depending on whether the freestream perturbations consist of a standing wave or traveling waves. For standing-wave freestream conditions, there is a phase lead of the velocity in the inner layer, reaching a maximum value of 45 deg at high values of reduced frequency. For traveling-wave freestream conditions, two parameters, the reduced frequency $\bar{\omega}$ and the traveling-wave convection velocity ratio Q/U_0, are required to fully describe the flow. With a freestream subject to traveling waves and with Q/U_0 less than about 2.0, the boundary-layer velocity exhibits a phase lag with respect to the freestream that increases with decreasing values of Q/U_0. The calculation method can be extended to turbulent boundary layers subject to traveling waves by incoporating the eddy viscosity model of Cebeci and Carr.

Acknowledgments

The author is grateful to the Director, staff, and students of the Whittle Laboratory, Cambridge University Engineering Department, for many helpful discussions during the preparation of this Note.

References

[1]Evans, R. L., "Boundary Layer Development on an Axial-Flow Compressor Stator Blade," *ASME Journal of Engineering for Power*, Vol. 100, April 1978, pp. 287-293.

[2]Cebeci, T. and Carr, L. W., "A Computer Program for Calculating Laminar and Turbulent Boundary Layers for Two-Dimensional Time-Dependent Flows," NASA TM-78470, March 1978.

[3]Lighthill, M. J., "The Response of Laminar Skin Friction and Heat Transfer to Fluctuations in the Stream Velocity,' *Proceedings of the Royal Society of London*, Vol. 224A, 1954, pp. 1-23.

[4]Patel, M. H., "On Laminar Boundary Layers in Oscillatory Flow," *Proceedings of the Royal Society of London*, Vol. 347A, 1975, pp. 99-123.

[5]Evans, R. L., "Unsteady Laminar Boundary Layers Subject to Standing Wave or Traveling Wave Freestream Fluctuations," Cambridge Univ. Engineering Dept., Cambridge, England, Rept. CUED/A-Turbo/TR 124, 1988.

Shock-Wave/Boundary-Layer Interaction at a Swept Compression Corner

Oktay Özcan* and M. Orhan Kaya†
Istanbul Technical University, Istanbul, Turkey

Introduction

IN supersonic flow over a compression corner mounted on a flat plate, a shock wave is formed ahead of the compression corner. The adverse pressure gradient caused by the shock wave propagates upstream through the subsonic portion of the boundary layer developing on the flat plate. The interaction of the shock wave with the boundary layer can lead to flow separation if the shock wave is sufficiently strong. In the case of swept compression corners, the resulting interaction is too complex for significant analytical treatment, and, therefore, experimental data are necessary to understand the flow physics. Such data are reported by Refs. 1, 2, and 3. A numerical solution of the separated flow problem is given by Horstman.[4]

A sketch of the swept compression corner geometry is given in Fig. 1. The quantities α and λ are the compression angle and sweep angle, respectively. The separation angle β is defined as the angle between the separation line and the spanwise direction z. Settles and Teng[3] report the existence of two distinct flow regimes, which are referred to as cylindrical and conical. The separation line and the corner line make an angle with each other in the conical flow regime ($\beta \neq \lambda$), whereas the two lines are parallel in the cylindrical flow ($\beta = \lambda$). Settles and Teng[3] propose the "Shock Detachment Hypothesis," which states that the transition from the cylindrical flow to the conical flow regime is due to the detachment of the shock wave that is otherwise attached to the corner for small α and λ.

The present note reports results of an experimental study carried out at Mach numbers between 1.8 and 2.2. Data were obtained by oil flow visualization. A third flow regime was observed in addition to the cylindrical and conical flow regimes. The new regime reveals itself when the Mach number to the corner line (M_n) is around one. Results of the study lend support to the "Shock Detachment Hypothesis."

Experiments

The experiments were conducted in the 60×30 mm Trisonic Wind Tunnel at the Istanbul Technical University. This facility is a continuous tunnel operating at atmospheric stagnation conditions. The freestream Mach number was varied by changing the shape of the Laval nozzle upstream of the test section. The freestream Reynolds number per unit length was 12.7×10^6 (1/m) at Mach 2.2.

The model geometry is defined by the parameters α, λ, t, and L, which are shown in Fig. 1. The models were made of plexiglas ($t = 4$ mm, $L = 50$ mm) and were mounted on the side wall of the tunnel. Approximatley 30 models with various values of α and λ were used in the experiments. The thickness of the fully developed turbulent boundary layer on the tunnel side wall was approximately 8 mm at the test section. The fact that model thickness t was smaller than boundary layer thickness δ was an interesting feature of the present study. In all previous studies of the flow t was larger than δ and the interaction was "dimensionless," that is, the model thickness did not impose a length dimension on the interaction characteristics. The interaction of the present study was probably dimensional. However, this was not verified by varying the model thickness systematically.

Oil flow visualization was made to observe the topology of the skin-friction line pattern on the flat plate. A mixture of titanium dioxide, oleic acid, and engine oil was used in oil flow visualization. The separation angle (β) was measured from the oil flow photographs taken during a tunnel run with an accuracy of $\pm$ one degree.

Discussion of Results

Oil flow visualization revealed three characteristic flow regimes. Figure 2 gives a schematic description of the flow

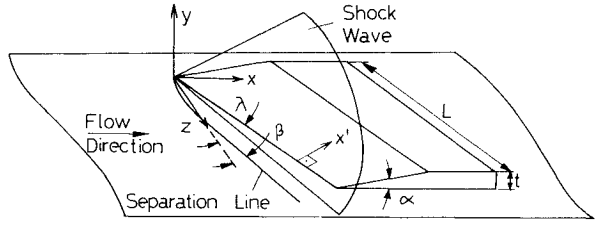

Fig. 1 A schematic view of the swept compression corner geometry.

Received Jan. 5, 1989; revision received March 20, 1989. Copyright © 1989 by American Institute of Aeronautics and Astronautics, Inc. All rights reserved.

*Associate Professor, Faculty of Aeronautics and Astronautics; currently Senior NRC Associate at NASA-ARC, CA. Member AIAA.

†Graduate Student, Faculty of Aeronautics and Astronautics.